Materials Science and Engineering A 496 (2008) 425–433

Contents lists available at ScienceDirect

Materials Science and Engineering A

journal homepage: www.elsevier.com/locate/msea

Effect of pre-aging and Al addition on age-hardening and microstructure in Mg-6 wt% Zn alloys

K. Oh-ishi[a,*], K. Hono[a], K.S. Shin[b]

[a] *National Institute for Materials Science (NIMS), 1-2-1 Sengen, Tsukuba 305-0047, Japan*
[b] *Magnesium Technology Innovation Center, RIAM, School of Materials Science and Engineering, Seoul National University, 599 Gwanangno, Gwanak-gu, Seoul 151-744, Republic of Korea*

ARTICLE INFO

Article history:
Received 29 March 2008
Received in revised form 26 May 2008
Accepted 2 June 2008

Keywords:
Age-hardening
Precipitation
G.P. zone
Transmission electron microscopy
Three-dimensional atom probe

ABSTRACT

The age-hardening response and microstructural variation Mg–Zn and Mg–Zn–Al alloys were examined by hardness test, transmission electron microscopy (TEM) and three-dimensional atom probe. The samples were prepared by hot-extrusion after casting. The two-step aged samples exhibit enhanced age-hardening response at an earlier stage compared to the single-aged ones. TEM observations exhibited that the peak aged Mg–Zn samples had two kinds of precipitates: one was a rod along the *c*-axis of the matrix phase; the other was a plate lying on the basal plane. The Mg–Zn–Al samples had rods and cuboidal precipitates. After two-step aging, the microstructure becomes finer for both the Mg–Zn and Mg–Zn–Al alloys. The rod-like precipitates were dominant in the peak aged Mg–Zn alloy, while the comparable number of rods and cuboidal precipitates were present in the Mg–Zn–Al alloy. Atom probe analyses for the samples pre-aged at 70 °C clearly showed the formation of Zn-rich zones.

1. Introduction

Recent thrust for weight reduction of automobiles and other transportation vehicles have made Mg alloys very attractive as structure materials. However, poor formability at room temperature and low high temperature strength make the use of Mg alloys limited to the components that can be produced by casting. Refinement of grain size and control of texture lead to improvements of formability and strength [1–4], and the addition of rare earth elements lead to the development of creep resistant alloys [5,6]. To broaden the applications of magnesium alloys further, the development of wrought Mg alloys with higher strength is necessary.

Mg–Zn alloys are most widely used wrought magnesium alloys, which is a basic composition of ZK series commercial alloys. Since the Mg–Zn alloy system is age-hardenable, there is a great potential to improve the strength by various heat treatments and micro-alloying. The studies on age-hardening and microstructure in this Mg–Zn alloy system have been carried out since 1960s [7–13], and the precipitation sequence is well documented starting from the Guinier Preston (G.P.) zone formation, followed by the formation of β_1' and β_2' precipitates, before reaching to the formation of an equilibrium β phase. The β_1' phase forms at the beginning of aging, then transforms to the β_2' with aging time. At the aging temperature above 110 °C, which is beyond the solvus of G.P. zone, the formation of G.P. zone is excluded. The transition phases of the β_1' and β_2' have been designated as a MgZn phase having a similar structure to $MgZn_2$ [7]. But they have different orientation relationships with the α-Mg matrix, which is $(0\,0\,0\,1)_\alpha//(1\,1\,\bar{2}\,0)_{\beta 1'}$, $[1\,1\,\bar{2}\,0]_\alpha//[0\,0\,0\,1]_{\beta 1'}$ and $(0\,0\,0\,1)_\alpha//(0\,0\,0\,1)_{\beta 2'}$, $[1\,0\,\bar{1}\,0]_\alpha//[1\,1\,\bar{2}\,0]_{\beta 2'}$, respectively [9,10,13]. Recently, some of researchers reported that the β_1' phase has a monoclinic structure similar to that of Mg_4Zn_7, but not that of $MgZn_2$ which has been believed till now [14,15]. Although the morphology and the crystal structure of these transition phases have been well characterized using transmission electron microscopy (TEM), the understandings of the G.P. zones that are believed to form in the pre-precipitation stage, remain limited because they were studied only by X-ray experiments and electrical resistivity measurements in the 1960s.

The age-hardening of Mg–Zn alloys has been known to be promoted by the addition of Ag, Ca or rare earth elements [13,16–18]. In addition, two-step aging (high temperature aging after pre-aging at a lower temperature) was reported to be very effective to refine the microstructure of Mg–Zn alloys [9,16,19]. Recently, Park et al. [16] reported that the Mg–Zn–Ag alloys with double aging treatments exhibit higher strengths than single-aged alloys. Further recently, microstructure and mechanical properties of twin-roll strip Mg–6Zn–1Mn (wt%) alloys containing various Al contents subjected to double aging after solution heat treatment have been reported [19]. According to that, Mg–6Zn–1Mn–1Al (wt%) alloy

---

[*] Corresponding author. Tel.: +81 29 859 2752; fax: +81 29 859 2701.
E-mail address: oishi.keiichiro@nims.go.jp (K. Oh-ishi).

0921-5093/$ – see front matter © 2008 Elsevier B.V. All rights reserved.
doi:10.1016/j.msea.2008.06.005

has been shown to exhibit excellent tensile properties because of refined precipitates by Al addition. But the detailed microstructure analysis, in particular at the pre-aging condition, has not been conducted yet. The objective of the present work is to investigate the age-hardening response and resulting microstructure of Mg–Zn and Mg–Zn–Al alloys that are subjected to two-step aging by using TEM and three-dimensional atom probe (3DAP).

2. Experimental procedures

Billets with nominal alloy compositions of Mg–6Zn–1Mn and Mg–6Zn–3Al–1Mn (wt%) or Mg–2.3Zn–0.5Mn and Mg–2.3Zn–2.8Al–0.5Mn (at%) were prepared by gravity casting. Hereafter, they are designated as ZM61 and ZAM631 following commercial nomenclatures, respectively. Samples were extruded at 350 °C with an extrusion ratio of 25 and a ram speed of 0.4 mm/s. These extruded bars were homogenized at 400 °C for 12 h and quenched into ice water. The homogenized samples were artificially aged at 70 and 150 °C. A two-step aging was carried out by pre-aging at 70 °C for 48 h, followed by aging at 150 °C. Hardness measurements were performed by a micro-Vickers apparatus under a load of 50 g.

TEM specimens were prepared by the twin-jet polishing technique using a solution of 5.3 g LiCl, 11.16 g Mg(ClO$_4$)$_2$, 500 ml methanol, and 100 ml 2-butoxy-ethanol at about −50 °C and 90 V. Some of the specimens were finished for surface cleaning by ion milling using a Gatan Precision Ion Polishing System (PIPS) at an operating voltage of 2 kV for ∼20 min. Microstructure analyses were conducted using Philips CM200 and TECNAI G^2 F30 TEMs. An elemental mapping was obtained by the Gatan Imaging Filter Tridium equipped on the TECNAI G^2 F30 TEM. The jump ratio method was employed to obtain energy filtered maps. The thickness of TEM foils for number density calculations was determined using convergent-beam electron diffraction analysis [20]. Atom probe analyses were performed using a three-dimensional atom probe (3DAP) equipped with the CAMECA tomographic atom probe (TAP) detection system. The field evaporation was assisted by femtosecond laser pulse (400 fs, 55 μJ/mm^2) to avoid specimen rupture, at a sample temperature of ∼30 K in an ultra-high vacuum condition. Needle-like atom probe specimens were prepared by the micro-polishing technique.

3. Results

Fig. 1 shows aging curves of the materials subjected to single aging at 70 and 150 °C and two-step aging at 150 °C. No age-hardening is observed at 70 °C for both the ZM61 and ZAM631 alloys. During the aging at 150 °C, the hardness of the alloys increases with time and reaches a peak hardness after ∼96 h. The age-hardening of two-step aged samples starts earlier than that of the single-aged ones, and the peak hardness of the ZAM631 is higher than that of the ZM61. After passing the peak, the decrease of hardness due to overaging is not so evident. The tendency of age-hardening for both alloys is similar except that the base hardness of the ZAM631 sample is higher by about $H_V \sim 13$. This suggests that Al mainly contribute to the solid solution hardening.

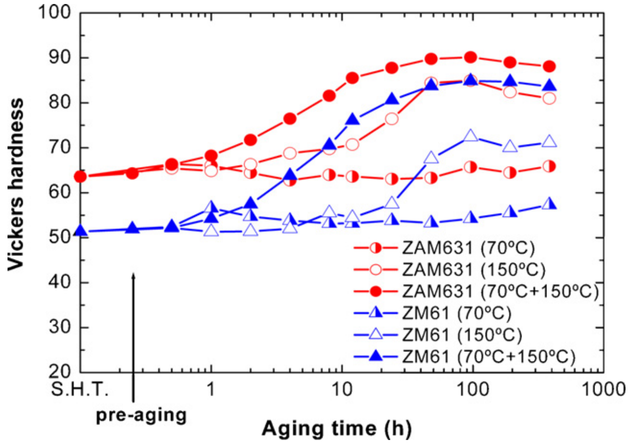

Fig. 1. Aging curves of ZM61 and ZAM631 alloys subjected to single aging at 70 and 150 °C and two-step aging at 150 °C.

Fig. 2 shows (a) a bright field (BF) TEM image and (b) a high resolution TEM image of the ZAM631 sample aged at 70 °C for 48 h, taken from the [0 0 0 1] zone axis. This corresponds to the pre-aged condition of the two-step aging. In Fig. 2(a) fine particles (∼5 nm) having dark contrast are observed with a very high number density (∼1.6 × 10^{22}/m^3) and some of them are observed along the dislocation in the $[1\bar{1}00]$ direction. Particle alignments along the $\langle 1\bar{1}00\rangle$ directions are observed from place to place. The high resolution TEM image (Fig. 2(b)) shows spherical precipitate having ∼5 nm in size. Clear lattice contrast cannot be seen inside the particle, even though it was imaged with different defocusing conditions. Furthermore, the SAED pattern inset in Fig. 2(a) as well as the fast Fourier transform (FFT) pattern obtained from the particle did not exhibit any extra spots and streaks. In Mg–Zn binary alloys Mima and Tanaka [11,12] proposed the C-curves obtained from the aging curves of electrical resistance and hardness, which represent variation of phases, such as G.P. zones or pre-β', as a function of

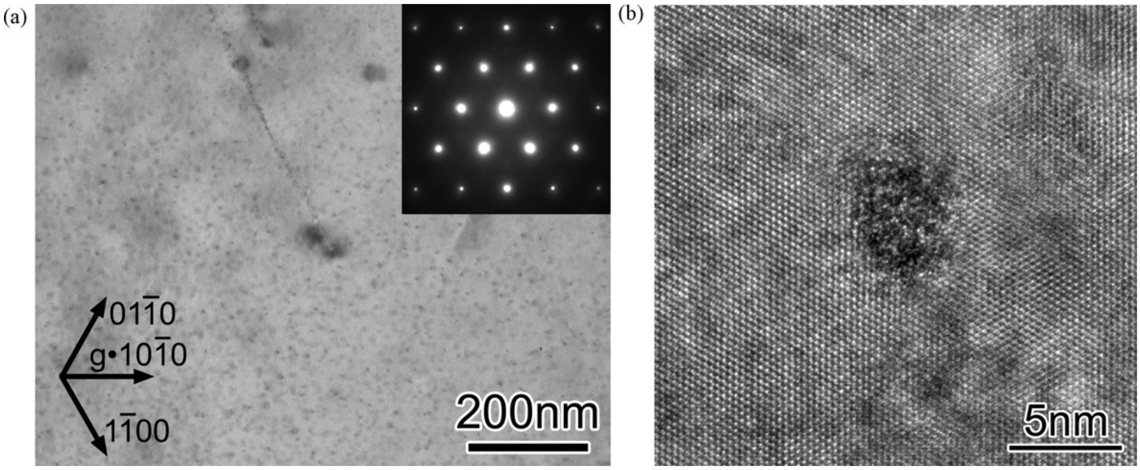

Fig. 2. (a) BF image and (b) high resolution TEM image for ZAM631 aged at 70 °C for 48 h, taken from the [0 0 0 1] zone axis.